

# Direct Conversion of Bulk Metals to Size-Tailored, Monodisperse Spherical Non-Coinage-Metal Nanocrystals\*\*

Rui-Chun Luo, Chao Li, Xi-Wen Du, and Jing Yang\*

**Abstract:** Monodisperse non-noble metal nanocrystals (NCs) that are highly uniform in shapes and particle size are much desired in various advanced applications, and are commonly prepared by either thermal decomposition or reduction, where reactive organometallic precursors or/and strong reducing agents are mandatory; however, these are usually toxic, costly, or suffer a lack of availability. Bulk Group 12 metals can now be converted into ligand-protected, highly crystalline, monodisperse spherical metal NCs with precisely controlled sizes without using any precursors and reducers. The method is based on low-power NIR-laser-induced size-selective layer-by-layer surface vaporization. The monodisperse Cd NCs show pronounced deep-UV (DUV) localized surface plasmon resonance making them highly competitive DUV-plasmonic materials. This approach will promote appreciably the emergence of a wide range of monodisperse technically important non-coinage metal NCs with compelling functionalities.

**M**etal nanocrystals (NCs) are of particular importance in nanoscience and technology owing to their unique electrical, optical, magnetic, and catalytic properties, rendering them highly desirable in numerous state-of-the-art applications such as high-performance Li-ion batteries,<sup>[1]</sup> high-density renewable energy storage,<sup>[2]</sup> surface-enhanced Raman spectroscopy (SERS),<sup>[3]</sup> localized surface plasmon resonance (LSPR) sensors,<sup>[4]</sup> and theranostic probes.<sup>[5]</sup> To succeed in the above applications, metal NCs in general ought to be made monodisperse with very narrow distribution in both dimension and morphology owing to the significant size and shape effects.<sup>[1,5–8]</sup> Monodisperse colloidal metal NCs have also been regarded as ideal building units for advanced superstructures and devices.<sup>[9]</sup> To date, several colloidal chemistry methods have been developed to synthesize monodisperse spherical metal NCs with controlled particle sizes.<sup>[1,10–12]</sup> It is well-known that the colloidal chemistry is based on a bottom-up strategy, where the neutral metal atoms

need to be firstly released through either reduction or thermolysis of the precursors to initiate nucleation and subsequent growth of metal NCs. Owing to the intrinsic inertness, noble metal NCs, such as Au and Pt, can be easily prepared by reduction of metal salts with alcohols.<sup>[10]</sup> In contrast, for the synthesis of non-noble metal NCs, reactive organometallic precursors (that is, metal carbonyls, metal amides) or/and strong reducing agents (that is, superhydride, sodium borohydride) are prerequisite,<sup>[1,11,12]</sup> however, these are usually hazardous, costly, complex, and even lack availability.

Herein, for the first time, we report on a robust conversion strategy, free of precursors and reducing agents, which transforms bulk non-noble metals directly into ligand-protected, size-tailored, highly crystalline, monodisperse spherical non-noble metal NCs, by low-power nanosecond NIR-laser ablation/irradiation. This top-down route is distinct from what we developed previously for monodisperse quantum dots based on the quantum confinement effect,<sup>[13]</sup> since the bandgaps are not size-tunable in metal NCs larger than 1 nm. Group 12 metals are chosen as particular examples here, since Cd and Zn NCs can be utilized as intermediates in the synthesis of high-performance optoelectronic and optical nanostructured Group 12–16 (II–VI) compounds, such as CdS, ZnO, and so on. For instance, Alivisatos and co-workers prepared hollow CdS spheres by sulfidation of submicrometer-sized spherical Cd crystals based on the nanoscale Kirkendall effect,<sup>[14]</sup> and the hollow CdS spheres were found to possess ultrahigh stress and strain.<sup>[15]</sup> Nevertheless, to the best of our knowledge, size-tailored monodisperse Cd and Zn NCs smaller than 100 nm have never been reported. Herein, we convert directly bulk Cd (or Zn) into oleic acid (OA)-protected monodisperse ( $\sigma < 10\%$ ) spherical Cd (or Zn) NCs with high crystallinity and controllable particle sizes 6.5–16.8 nm by varying the laser fluence. Furthermore, the monodisperse Cd NCs colloid exhibits pronounced LSPR in the DUV spectral regime.

It is noteworthy that much effort has been devoted in size-reduction and size-distribution-narrowing of polydisperse noble metal NCs by laser irradiation in liquid (LIL); however, monodisperse particles ( $\sigma < 10\%$ ) with controllable sizes have never been achieved.<sup>[16–18]</sup> Our method manifests itself as innovative based on the following two aspects: 1) In conventional LIL, lasers with wavelengths in the visible and UV region where the photon energy are absorbed strongly by metals were usually adopted, resulting in complete vaporization of metal NCs, thus giving rise to uncontrollable polydisperse particles.<sup>[16–18]</sup> In contrast, in our work, a low-power nanosecond NIR nanosecond laser is used to enable moderately photothermal heating for the metal NCs and

[\*] R.-C. Luo, C. Li, Prof. X.-W. Du, Prof. J. Yang  
Institute of New-Energy Materials, Tianjin Key Laboratory of Composite and Functional Materials, School of Materials Science and Engineering, Tianjin University  
92 Weijin Road, Nankai District, Tianjin 300072 (China)  
E-mail: yang\_jing@tju.edu.cn

[\*\*] This work was supported by the Natural Science Foundation of China (No. 51271129), Natural Science Foundation of Tianjin City (No. 14JCYBJC17200), Program for New Century Excellent Talents in University (No. NCET-13-0414), National Key Basic Research Program of China (2014CB931703), and Seed Foundation of Tianjin University.

Supporting information for this article is available on the WWW under <http://dx.doi.org/10.1002/anie.201411322>.

thereby realizes controllable size-selective layer-by-layer surface vaporization (SLSV) of NCs, which facilitates a good size control. 2) In contrast to previous work, we add a defined amount of OA (ca. 1.0 mM) into the organic solvent for laser ablation/irradiation, which was found to contribute greatly in achieving a high monodispersity in particle sizes.

In a typical conversion process (Supporting Information, Figure S1), parts of the Cd plate (Figure 1a) was first turned into polydisperse spherical CdNCs (40–80 nm, named raw NCs hereafter; Figure 1b) by laser ablation, and further converted dramatically into spherical NCs with a high size-uniformity (Figure 1c–f) following laser irradiation of the raw NCs colloids. The CdNCs self-assemble into ordered two-dimensional superlattices on the carbon grids, suggesting a high monodispersity of the particles. A high-resolution TEM (HRTEM) image (Figure 1g) confirms the highly crystalline nature of NCs, with a lattice spacing of 0.279 nm corresponding to (100), ( $\bar{1}$ 10), and (010) planes of hexagonal Cd, and the fast Fourier transform (FFT) image (inset of Figure 1g) indicates a hexagonal structure with [0001] orientation. The selected-area electron diffraction (SAED) pattern (Figure 1h) is also indexed well to a hexagonal structure of bulk Cd. The as-prepared spherical CdNCs are of high monodispersity with size dispersion 6.5–9.5% without post size-selective precipitation procedures. The particle sizes can be tuned precisely between 6.5–16.8 nm, decreasing monochromatically with laser fluence (Figure 1i and j). Fourier transform infrared (FTIR) measurements reveal that the monodisperse CdNCs are stabilized by a monolayer of OA molecules chemisorbed on the particle surface in a bridging bidentate manner (Supporting Information, Figure S2). As a strongly binding capping agent, OA not only

stabilizes colloidal NCs, but also passivates metal NCs against fast oxidation owing to the close-packed monolayer of coordinating ligand.<sup>[19]</sup> Meanwhile, direct conversion of a piece of Zn plate to monodisperse colloidal ZnNCs with high crystallinity and tunable size, that is, 15.8 nm ( $\sigma = 9.6\%$ ) and 11.0 nm ( $\sigma = 10.2\%$ ), were also achieved successfully by performing similar procedures (Supporting Information, Figure S3). The particle surfaces appear a little fuzzy, which is probably due to the fast surface oxidation of highly reactive metal NCs before TEM observation.

Polydisperse metal NCs have been commonly obtained by laser ablation of metal plates in liquids.<sup>[20]</sup> However, they are usually linked and agglomerated (Supporting Information, Figure S4a), or even coated with amorphous carbon when using inert organic solvents as liquid media (Supporting Information, Figure S4b), that is, cyclohexane in our study, to keep reactive metal NCs from oxidation during synthesis. Further laser irradiation of these particles resulted in polydisperse NCs (Supporting Information, Figure S4c) mixed with carbon species (Figure S4d). Interestingly, incorporating a tiny amount of OA (ca. 0.4 mM) into the liquid for laser ablation led to well-dispersed spherical NCs without any carbon capping on the surfaces (Figure 1b, inset). This could be ascribed to the high affinity between OA and the metal nanoparticles<sup>[19]</sup> and the high decomposition temperature of OA. The OA coating (Supporting Information, Figure S2) could effectively screen off the low-decomposition-temperature organic solvent from the hot metal nanodroplets ejected from the metal plate, and thus prevents it from thermally decomposing into amorphous carbon.

To investigate how these well-dispersed raw NCs transform into monodisperse particles upon laser irradiation, we

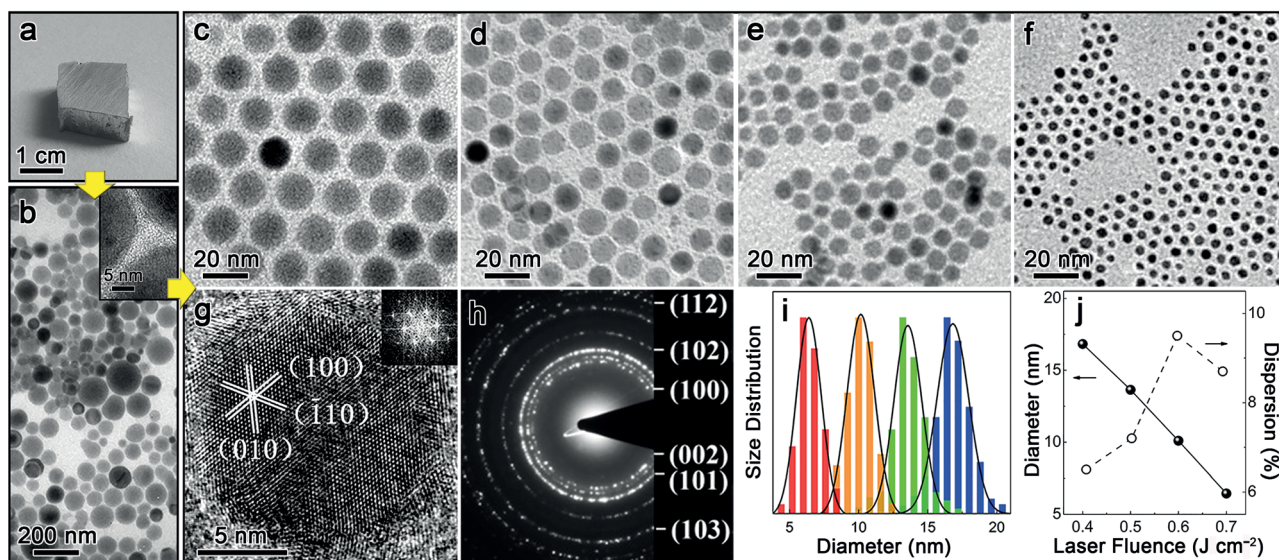


**Figure 1.** Size-tailored monodisperse colloidal Cd NCs prepared directly from a piece of Cd plate, based on laser ablation/irradiation in liquid. a) Photograph of the Cd plate. b) TEM image of polydisperse Cd NCs obtained by laser ablation of the Cd plate. Inset: a high-resolution TEM (HRTEM) image of the particle surface. c)–f) TEM images of monodisperse Cd NCs with controllable sizes 16.8–6.5 nm, prepared by laser irradiation of the NCs shown in (b) with different laser fluence ( $0.4\text{--}0.7\text{ J cm}^{-2}$ ). g) HRTEM image of one Cd NC shown in (c), viewed along the direction [0001]. Inset: the corresponding fast-Fourier transform pattern. h) Selected-area electron diffraction pattern of Cd NCs shown in (c). i) Size histograms ( $\sigma \approx 6.5, 7.2, 9.5$ , and  $8.7\%$  for 16.8, 13.6, 10.1, and 6.5 nm NCs, respectively) with Gaussian fitting. j) Dependence of the NC mean diameter and size dispersion on laser fluence.

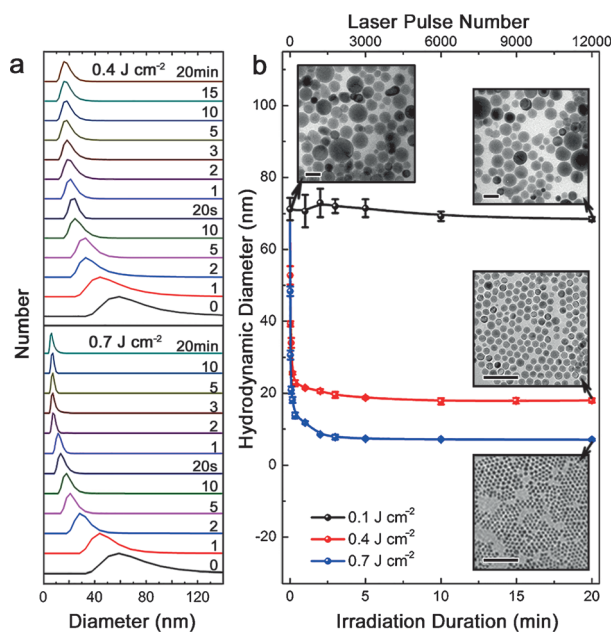


**Figure 2.** a) Variation of CdNC size distribution with laser irradiation up to 20 min, for laser fluence  $J_0 = 0.4 \text{ J cm}^{-2}$  and  $J_0 = 0.7 \text{ J cm}^{-2}$ , respectively. b) NCs mean diameters as functions of laser irradiation time for  $J_0 = 0.1, 0.4, 0.7 \text{ J cm}^{-2}$ . Error bars represent the measurement error. Scale bars are 100 nm.

studied the size distribution evolution by adopting a DLS technique. As seen in Figure 2a, the initial NCs are fairly large and distribute broadly in size. As laser irradiation prolongs, the mean diameter of NCs reduces, and the size distribution also becomes progressively narrower. During the first 20 s of laser irradiation (equivalently 200 pulses), the mean particle size decreases rapidly from 70 nm to 20 nm and 15 nm for laser fluence  $J_0 = 0.4 \text{ J cm}^{-2}$  and  $0.7 \text{ J cm}^{-2}$ , respectively (Figure 2b). Thereafter, the size-reduction proceeds more slowly and finally terminates with steady diameters of 18.0 nm and 7.0 nm for  $J_0 = 0.4 \text{ J cm}^{-2}$  and  $0.7 \text{ J cm}^{-2}$ , respectively, following 20 min of irradiation. The hydrodynamic sizes obtained in DLS are slightly larger than the actual particle diameters in TEM arising from the decelerated Brownian motion caused by the coating of OA molecules on particle surfaces. However, for much lower laser fluences, namely  $J_0 = 0.1 \text{ J cm}^{-2}$ , the mean particle size hardly changes with irradiation and the initial polydisperse NCs remain intact following 20 min of laser irradiation (Figure 2b).

The size reduction of the non-uniform metal NCs upon nanosecond laser irradiation has been extensively studied<sup>[16–18]</sup> and ascribed to the partial or complete vaporization of NCs by laser pulses; nevertheless, highly uniform NCs have not yet been obtained. According to the heating–melting–vaporization model,<sup>[21]</sup> we theoretically calculated the lowest laser fluence ( $J^*$ ) needed for surface and complete vaporization of CdNCs with different sizes (Figure 3; see the Supporting Information for detailed calculations). It turns out that the experimentally derived mean particle sizes at different laser fluences coincide well with the theoretical curve of surface vaporization, suggesting that the layer-by-layer surface vaporization of NCs should be responsible for the size

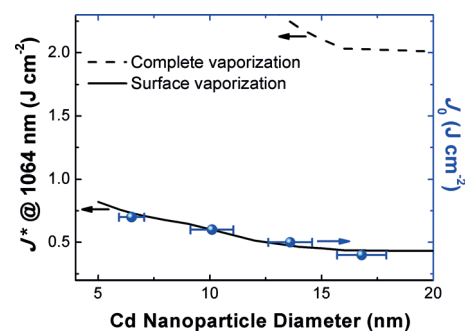


**Figure 3.** Theoretically calculated laser fluence threshold ( $J^*$ ) of surface and complete vaporization of Cd NPs with different sizes, and experimentally derived NP mean diameter for different laser fluence ( $J_0$ ).

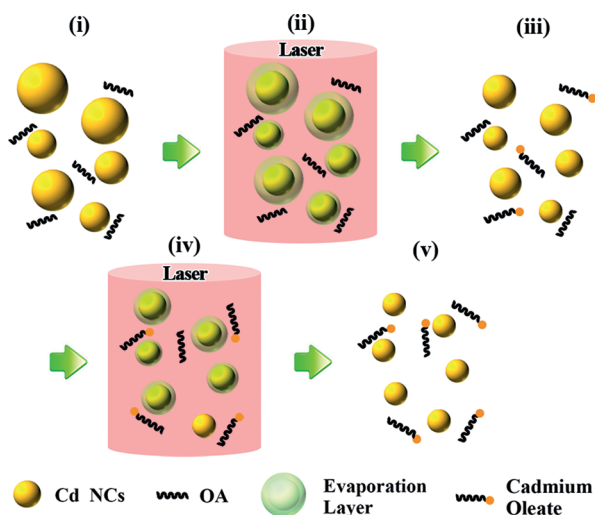
reduction in our study, and the smallest size of particles that could be barely vaporized by the NIR laser beam gives the steady particle size  $D^*$ . For a given  $J_0$ , as the lowest laser fluence needed for surface vaporization of initial particles with  $D \gg D^*$  much lower than that provided (Figure 3), the initial NCs will vaporize intensively from the surface and reduce their sizes abruptly, consistent with the observation in DLS (Figure 2b). As  $D$  decreases and approaches  $D^*$ , the particle size reduction becomes much slower, for  $J_0$  closer to the threshold of surface vaporization. Finally, when  $D$  reaches  $D^*$ , surface vaporization stops and size reduction terminates. It is noteworthy that because metals usually have relatively low absorption efficiency in NIR, the adoption of first harmonic nanosecond laser irradiation guarantees moderately photothermal heating for the metal particles, giving rise to controllable SLSV of NCs, in contrast to unpredictable size manipulation owing to complete vaporization of metal NCs by visible or UV lasers usually adopted in conventional LIL.

Last but not least, the question arises as to where the free Cd atoms arising from surface vaporization of NCs have gone. It is surprising to note that, in the controlled experiments, if the amount of OA added before laser irradiation was reduced to one tenths of the original amount, polydisperse NCs with a bimodal size distribution resulted, where smaller NCs (mean diameter 4.5 nm) emerging along with the monodisperse NCs ( $16.8 \pm 1.1 \text{ nm}$ ), following laser irradiation at  $J_0 = 0.4 \text{ J cm}^{-2}$  (Supporting Information, Figure S6a,b). Conversely, if excess OA were added, irregular-shaped NCs with a wide size distribution appeared owing to surface etching (Supporting Information, Figure S6c,d). Consequently, an appropriate amount of OA is extremely vital in achieving a high monodispersity of NCs. Numerous infrared studies have shown that the carboxylate ion could coordinate to a metal atom to form metal complexes of carboxylic acids.<sup>[22]</sup> In this work, an proper amount of OA guarantees that all of the surface-vaporization-released Cd atoms could completely coordinate to the oleate ions to form cadmium oleate molecules as revealed by the FTIR measurements (Supporting Information, Figure S7, and detailed discussion therein). Owing to the selective heating mechanism of the pulsed nanosecond laser, the temperature of cyclohexane stays at room temperature during laser irradiation. Therefore, cadmium oleate molecules could be dispersed stably in cyclo-



hexane, avoiding the generation of smaller particles with unpredictable sizes owing to additional nucleation and growth of the free Cd atoms. With much less OA, the amount of oleate ions are not enough to coordinate to all of the free Cd atoms (Supporting Information, Figure S7), leading to the formation of NCs with uncontrolled sizes owing to the condensation of remaining free Cd atoms (Supporting Information, Figure S6a,b).

On account of the above, the conversion process of polydisperse Cd NCs to monodisperse Cd NCs is summarized in Scheme 1. Under NIR nanosecond laser irradiation with



**Scheme 1.** Illustration of the conversion process of polydisperse Cd NCs to monodisperse Cd NCs based on size-selective layer-by-layer surface vaporization.

certain fluence, the initial polydisperse NCs with sizes much larger than  $D^*$  vaporize abruptly from the surface, while those smaller sizes vaporize slightly (i→ii). Besides, the vaporization-released Cd atoms will coordinate to the OA molecules, giving rise to effective size distribution narrowing of NCs under repetitive laser pulses (ii→iii→iv). Finally, after irradiation with thousands of pulses, the particle sizes become equal to or slightly smaller than  $D^*$ , and therefore SLSV terminates and monodisperse NCs result (iv→v).

The as-prepared monodisperse colloidal Cd NCs exhibits strong LSPR located at 280 nm, which is well within the DUV spectral regime (Figure 4a), consistent with the FDTD simulations (Figure 4b). It should be noted that the LSPR peak can be barely tuned by varying the particle sizes between 6.5–16.9 nm. The pronounced calculated extinction efficiency (ca. 3.3 at photon energy 4.4 eV for 16.9 nm Cd NCs) makes Cd NCs highly competitive DUV-plasmonic materials,<sup>[23]</sup> and thus are greatly important to SERS and SERRS, which are useful in surface science, catalysis science, electrochemistry, and materials research<sup>[24]</sup> because with DUV excitation, the Raman scattering cross-section and the signal-to-noise ratio of the Raman spectra will be significantly enhanced.<sup>[25]</sup> Moreover, it was recently reported by Li and co-workers that a thin layer of silica or alumina coating on Au nanoparticles did not alter their plasmonic behavior much.<sup>[26]</sup>

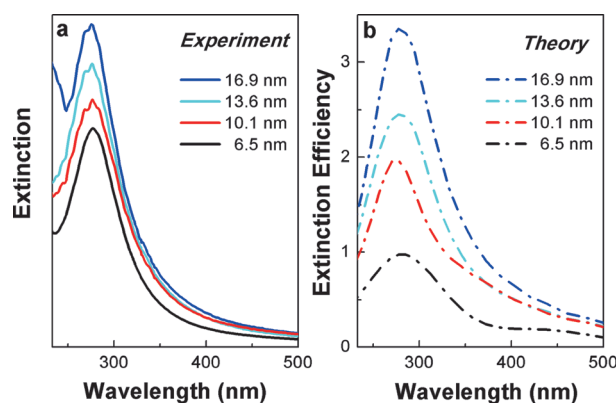


**Figure 4.** a) Experimental UV/Vis extinction spectra of the monodisperse Cd NC colloids with different particle size. b) Theoretical extinction efficiency spectra calculated by using FDTD simulations.

Therefore, coating Cd NCs with a thin layer of silica or alumina might be a possible solution to diminish effectively their hazard to the environment for applications in DUV-SERS or DUV-SERRS, because the thin silica layer was found to have little effect on the DUV-plasmonic behavior of the Cd NCs (Supporting Information, Figure S9). Besides, the LSPR peak will move to deeper UV region if water or air served as the media.

In conclusion, we have developed a novel top-down conversion strategy that is completely different from the conventional methods (namely, reduction and thermal decomposition), for the preparation of monodisperse noble metal NCs. In our synthetic route, bulk Group 12 metals are converted directly into ligand-protected, size-tailored, highly crystalline, monodisperse spherical metal NCs, without using any reducing agents and precursors. The conversion process should be attributed to the controllable size-selective layer-by-layer surface vaporization of the polydisperse metal NCs, induced by low power NIR-laser irradiation. Meanwhile, a proper amount of OA in the solution eliminates effectively additional particle formation with uncontrolled sizes. The monodisperse spherical Cd colloids exhibit pronounced DUV-LSPR, making them highly competitive DUV-plasmonic materials. We believe that this facial conversion approach not only greatly simplifies the preparation procedures, but also, more importantly, makes it possible to synthesis a large variety of monodisperse technically important non-coinage metal NCs that have been hardly implemented to date (for example, Al, Cr, Sb) with compelling functionalities.

## Experimental Section

General procedure for the preparation of monodisperse metal NCs: The first harmonic (wavelength 1064 nm) of a nanosecond pulsed Nd:YAG laser (Dawa-350, Beamtech; pulse width 7 ns, maximum output 350 W) was adopted. Typically, raw Cd (or Zn) NCs were first prepared by laser ablation (focused, repetition rate 5 Hz, ca. 60 mJ per pulse) of a piece of Cd (or Zn) (purity 99.99%) plate immersed in a solution of 25 mL of cyclohexane and 3  $\mu$ L of oleic acid (OA) with a 5 mm thick liquid layer for 20 min (Supporting Information, Figure S1). Second, 8 mL of the as-prepared colloid was transferred

to a quartz tube, mixed with 3  $\mu\text{L}$  of OA, and then irradiated by the unfocused laser (10 Hz, 0.4–0.7  $\text{J cm}^{-2}$  per pulse) for 20 min. All of the laser treatments were performed under argon protection and vigorous stirring with a magnetic stirrer.

**Characterization:** TEM images are obtained by using an FEI Technai G2 F20 transmission electron microscope equipped with a field-emission gun. Infrared spectra of samples were recorded using a Bruker Tensor 27 FTIR spectrometer in the range of 400–4000  $\text{cm}^{-1}$ . The DLS measurements were performed at 25  $^{\circ}\text{C}$  with Malvern Zetasizer Nano ZS90. Extinction spectra were taken using a Hitachi U-4100 spectrophotometer.

**Simulation:** The extinction efficiency, which is the ratio of the extinction cross-section to the nanosphere area, was calculated using the finite difference time domain method (FDTD, Lumerical) for spherical NCs covered by a monolayer of OA molecules (refractive index  $n = 1.46$ ) with thickness of 2.5 nm,<sup>[27]</sup> embedded in the medium of cyclohexane ( $n_{\text{medium}} = 1.43$ ). A normal incidence plane wave was applied, and the complex refractive indices of Cd were specified using tabulated values.<sup>[28]</sup>

**Keywords:** laser irradiation · metal nanocrystals · monodisperse materials · plasmon resonance

**How to cite:** *Angew. Chem. Int. Ed.* **2015**, *54*, 4787–4791  
*Angew. Chem.* **2015**, *127*, 4869–4873

- [1] K. Kravchyk, L. Protesescu, M. I. Bodnarchuk, F. Krumeich, M. Yarema, M. Walter, C. Guntlin, M. V. Kovalenko, *J. Am. Chem. Soc.* **2013**, *135*, 4199.
- [2] C. W. Li, J. Ciston, M. W. Kanan, *Nature* **2014**, *508*, 504.
- [3] C. D. Andrea, J. Bochterle, A. Toma, C. Huck, F. Neubrech, E. Messina, B. Fazio, O. M. Maragò, E. Di Fabrizio, M. Lamy De La Chapelle, P. G. Gucciardi, A. Pucci, *ACS Nano* **2013**, *7*, 3522.
- [4] K. M. Mayer, J. H. Hafner, *Chem. Rev.* **2011**, *111*, 3828.
- [5] D. Ho, X. Sun, S. Sun, *Acc. Chem. Res.* **2011**, *44*, 875.
- [6] M. Green, *Chem. Commun.* **2005**, 3002.
- [7] G. Maidecchi, G. Gonella, R. Proietti Zaccaria, R. Moroni, L. Anghinolfi, A. Giglia, S. Nannarone, L. Mattera, H. Dai, M. Canepa, F. Bisio, *ACS Nano* **2013**, *7*, 5834.
- [8] I. Moreels, Y. Justo, B. De Geyter, K. Haestraete, J. C. Martins, Z. Hens, *ACS Nano* **2011**, *5*, 2004.
- [9] J. Fang, B. Ding, H. Gleiter, *Chem. Soc. Rev.* **2011**, *40*, 5347.
- [10] X. M. Lin, H. M. Jaeger, C. M. Sorensen, K. J. Klabunde, *J. Phys. Chem. B* **2001**, *105*, 3353.
- [11] T. Hyeon, *Chem. Commun.* **2003**, 927.
- [12] P. Zolotavin, P. Guyot-Sionnest, *ACS Nano* **2010**, *4*, 5599.
- [13] J. Yang, T. Ling, W. T. Wu, H. Liu, M. R. Gao, C. Ling, L. Li, X. W. Du, *Nat. Commun.* **2013**, *4*, 1695.
- [14] A. Cabot, R. K. Smith, Y. Yin, H. Zheng, B. M. Reinhard, H. Liu, A. P. Alivisatos, *ACS Nano* **2008**, *2*, 1452.
- [15] Z. W. Shan, G. Adesso, A. Cabot, M. P. Sherburne, S. A. Syed Asif, O. L. Warren, D. C. Chrzan, A. M. Minor, A. P. Alivisatos, *Nat. Mater.* **2008**, *7*, 947.
- [16] A. Takami, H. Kurita, S. Koda, *J. Phys. Chem. B* **1999**, *103*, 1226.
- [17] D. Werner, S. Hashimoto, T. Uwada, *Langmuir* **2010**, *26*, 9956.
- [18] V. Amendola, M. Meneghetti, *J. Mater. Chem.* **2007**, *17*, 4705.
- [19] N. Wu, L. Fu, M. Su, M. Aslam, K. C. Wong, V. P. Dravid, *Nano Lett.* **2004**, *4*, 383.
- [20] H. Zeng, X. W. Du, S. C. Singh, S. A. Kulinich, S. Yang, J. He, W. Cai, *Adv. Funct. Mater.* **2012**, *22*, 1333.
- [21] A. Pyatenko, M. Yamaguchi, M. Suzuki, *J. Phys. Chem. C* **2009**, *113*, 9078.
- [22] K. Nakamoto, *Infrared and Raman spectra of inorganic and coordination compounds*, 6th ed., Wiley, New York, **2009**.
- [23] J. M. Sanz, D. Ortiz, R. Alcaraz de La Osa, J. M. Saiz, F. Gonzalez, A. S. Brown, M. Losurdo, H. O. Everitt, F. Moreno, *J. Phys. Chem. C* **2013**, *117*, 19606.
- [24] B. Ren, X. F. Lin, Z. L. Yang, G. K. Liu, R. F. Aroca, B. W. Mao, Z. Q. Tian, *J. Am. Chem. Soc.* **2003**, *125*, 9598.
- [25] S. K. Jha, Z. Ahmed, M. Agio, Y. Ekinici, J. F. Löffler, *J. Am. Chem. Soc.* **2012**, *134*, 1966.
- [26] J. F. Li, X. D. Tian, S. B. Li, J. R. Anema, Z. L. Yang, Y. Ding, Y. F. Wu, Y. M. Zeng, Q. Z. Chen, B. Ren, Z. L. Wang, Z. Q. Tian, *Nat. Protoc.* **2013**, *8*, 52.
- [27] G. Konstantatos, I. Howard, A. Fischer, S. Hoogland, J. Clifford, E. Klem, L. Levina, E. H. Sargent, *Nature* **2006**, *442*, 180.
- [28] For 122–280 nm: T. M. Jelinek, R. N. Hamm, E. T. Arakawa, R. H. Huebner, *J. Opt. Soc. Am.* **1966**, *56*, 185; For 280–800 nm: A. P. Lenham, D. M. Treherne, *Proc. Phys. Soc.* **1964**, *83*, 1059.

Received: November 22, 2014

Revised: January 24, 2015

Published online: February 23, 2015